REVIEW: GEOLOGY

Oblique Stepwise Rise and Growth of the Tibet Plateau

Paul Tapponnier,[1]* Xu Zhiqin,[2] Françoise Roger,[1] Bertrand Meyer,[1] Nicolas Arnaud,[3] Gérard Wittlinger,[4] Yang Jingsui[2]

Two end member models of how the high elevations in Tibet formed are (i) continuous thickening and widespread viscous flow of the crust and mantle of the entire plateau and (ii) time-dependent, localized shear between coherent lithospheric blocks. Recent studies of Cenozoic deformation, magmatism, and seismic structure lend support to the latter. Since India collided with Asia ~55 million years ago, the rise of the high Tibetan plateau likely occurred in three main steps, by successive growth and uplift of 300- to 500-kilometer-wide crustal thrust-wedges. The crust thickened, while the mantle, decoupled beneath gently dipping shear zones, did not. Sediment infilling, bathtub-like, of dammed intermontane basins formed flat high plains at each step. The existence of magmatic belts younging northward implies that slabs of Asian mantle subducted one after another under ranges north of the Himalayas. Subduction was oblique and accompanied by extrusion along the left lateral strike-slip faults that slice Tibet's east side. These mechanisms, akin to plate tectonics hidden by thickening crust, with slip-partitioning, account for the dominant growth of the Tibet Plateau toward the east and northeast.

Tibet is Earth's largest and highest plateau, with a flat interior disrupted by active normal faulting (*1–6*) (Fig. 1). How such topography formed and is maintained has profound implications on the mechanics of continental deformation. Within the framework of India's collision with Asia, several models have addressed the question. One class of models focuses on today's uniform height (*3*), and on the extensional faulting, interpreted to indicate collapse of the plateau since the mid-Miocene (*7*) or earlier (*8*). The entire lithosphere is assumed to have thickened as a thin viscous sheet, with broadly distributed shortening of both crust and mantle having absorbed plate convergence (*9*, *10*). Tibet as a whole is then inferred to have risen significantly above its current altitude (~5000 m), as its crust buoyantly rebounded because of removal of part of its thickened lithospheric mantle, which triggered extension and volcanism (*9–11*). This "soft Tibet" model, however, ignores the half-dozen large strike-slip faults that border or slice the plateau, some of them at least as long as California's San Andreas fault (*12*), (Fig. 1). The existence of such first-order tectonic features and their association with the high topography, which is unlikely to be coincidental, thus remains to be explained.

Evidence from geological, geochronological, and seismic studies now shows that these fault zones, far from being shallow and late (and hence minor) side effects of thickening (*9*, *10*), have been key in controlling the growth of the Tibetan highlands from the start. Such studies also indicate little or no sign of lithospheric removal or surface rebound. Here, we review these recent findings and discuss an alternative model for the rise of topography north of the Himalayas that reconciles the two most prominent facets of Tertiary Asian tectonics: strike-slip extrusion and plateau building.

Strain and Faulting in Tibet

In Tibet, upthrust basement is only exposed along a few ranges (Gangdese, Tanggula, Kunlun, Altyn Tagh, and Qilian Shan) (Figs. 1 and 2) separated by large basins. Older, wide basins trend ~EW to NW-SE, parallel to the ranges. Younger, narrow ones trend NS. The youngest basins in southern Tibet and Yunnan are rifts due to ongoing, roughly EW extension (*1*, *2*, *12*) (Fig. 1). The total amount of extension related to the active normal faults of Tibet is quite small. As deduced from structural relief, it is at most a few tens of kilometers (≤40 km), less than 3% strain across the ~1200-km-long stretch of the plateau cut by the faults (~80 to 92E) (*1*, *2*, *10*). Most of the Tibetan rifts are filled with Plio-Quaternary conglomerates, and cut at high-angle older ~EW basins with Miocene deposits (*1*, *2*). Only the Thakkola and Yadong-Gulu grabens may have developed earlier (*13*, *14*), probably in connection with strike-slip along the Karakorum and Jiali faults, respectively (Fig. 1). Overall, the extension regime thus postdates the Miocene, and the corresponding amount of crustal thinning since is less than 2 km, negligible at the scale of the collision zone (*1*, *2*). Six of the young NS trending rifts (Fig. 1) extend across the Zangbo suture into the Greater Himalayas (*1*, *2*, *4–6*), a region underlain by flexed Indian-plate mantle (*15–17*), beneath which lithospheric thinning did not occur. Extension in southern Tibet is thus most simply interpreted to result from a combination of dextral slip-partitioning and divergent thrusting along the MFT (*1*, *2*, *18*). The shortening rate predicted from this interpretation is consistent with that measured across the Himalayas [~2 cm/year; (*19*, *20*)], which corroborates the small amount of extension across the southern plateau. More subdued normal faulting in northern Tibet seems to result also from strike-slip movement, particularly near the splaying SW ends of the sinistral (left-lateral) Kunlun and Altyn Tagh faults (*1*, *2*, *4–6*, *21–23*). In Yunnan, Pliocene-Quaternary extension is associated with bookshelf faulting due to horizontal shear (*1*, *2*, *12*, *24–27*), and occurs below 3000 m above sea level (a.s.l.). Thus, neither the kinematics and altitude, nor the timing and amount of normal faulting require a model in which extension might be driven by gravity collapse, itself triggered by wholesale rebound of a buoyant plateau to elevations ≥1 km higher than 5000 m in the Eocene or Mid-Miocene (*7–10*). Rather, the evidence at hand makes it likely that much more recent, if diachronous, extension in different areas was unrelated to large uplift increments (*14*, *18*, *28–30*). The coincidence of high topography with active normal faulting between about 28° and 36°N merely implies a large vertical stress that enhances rifting (*1*, *2*, *4–6*).

The great flatness of broad areas on the plateau has been taken to indicate a deficit of Tertiary shortening. But there is now ample field evidence to support the conclusion long derived from paleomagnetic inclination differences (*31*, *32*) that the amount of convergence absorbed since the Eocene by thrusts and strike-slip faults north and east of the Indus-Zangbo suture was large (~2000 km). North of the Kunlun Fault, in the Qaidam basin and Qilian Shan (Fig. 2), mass balance

[1]Institut de Physique du Globe, 4 Place Jussieu, 75252 Paris, France. [2]Ministry of Lands and Resources, Baiwanzhuang Rd, 100037 Beijing, China. [3]Universite Blaise Pascal, 5 rue Kessler, 63000 Clermont Ferrand, France. [4]EOST, Université Louis Pasteur, 5 rue Descartes 67084 Strasbourg, France.

*To whom correspondence should be addressed. E-mail: tappon@ipgp.jussieu.fr

estimates and retrodeformed sections across areas with predominantly Neogene deposits show at least 150 to 200 km of crustal shortening by thrusting in the last ~10 million years ago (Ma) (*28–30*). In the central part of the plateau, between the Kunlun and Tanggula ranges (Fenghuo Shan and Hohxil basin, Fig. 2), the strong folding, over a distance of ~300 km, of Paleogene red beds unconformably capped by more gently warped Neogene sandstones (*33–37*) implies a similar amount of earlier shortening. Comparable thrusting and folding affects the Eocene sandstones of the Lunpola and Baingoin basins (Fig. 2) south of the Tanggula range (*33–37*). Early-Middle Tertiary shortening also caused strong folding and thrusting of the Cretaceous-Paleocene red beds of the Chuxiong, Simao, and Lanping basins of Yunnan (*24–26*), and of the Nangqen and Qamdo-Markham basins south of Yushu in eastern Tibet (Fig. 2). At the southern edge of the Lhasa block, the Gangdese thrust alone appears to have absorbed more than 40 km of Oligocene shortening (*38*, *39*), and much of the folding of the Cretaceous sandstones and limestones north of the Gangdese and in NW Tibet may postdate 55 Ma (*40*, *41*). Burial by less deformed Cenozoic sediments in the undrained interior of the plateau, or erosional unroofing, leaving mostly pre-Cenozoic rocks in the east, make it difficult to estimate collision-driven crustal shortening with precision. But there is little reason to doubt that it was enough in most places (~50%) to raise the average elevation of Tibet to that presently observed.

Tertiary offsets on the two largest strike-slip faults of Tibet are now documented to exceed those of plate boundaries such as the San Andreas and Alpine Faults. For the Red River–Ailao Shan shear zone (Fig. 2), four independent lines of evidence—the 8° paleolatitude difference observed in Cretaceous red beds on either side (*42*), the reconstruction of seafloor-spreading in the South-China Sea (*43*), the concordant displacements of several Mesozoic geological markers, among which the Cretaceous granite belt along South China's rim (*24–26*), and the diachronous cooling of the exhumed Ailao Shan high-grade mylonitic gneisses (*44*)—show that the sinistral offset is most likely 700 ± 200 km (*24–26*). The ages of magnetic chrons (32 to 16 Ma) in the sea, a pull-apart basin at the end of the shear zone (*43*), and of crystallization and cooling of minerals in melts along the zone (35 to 15 Ma) (*24–26*, *44–46*) coincide, indicating that much of this offset accrued between the late Eocene and early Miocene at a rate of 3.5 to 4 cm/year. This rate is corroborated by the linear decrease in cooling ages along the Ailao Shan (~4 cm/year) (*44*). Sinistral shear was in large part coeval with transpressive thrusting and folding in the red-bed basins of Yunnan and SE Tibet, and both deformation regimes likely started before 35 Ma (*24–26*, *45–47*). On the Altyn Tagh Fault (Fig. 2), the separation between piercing points of the Early Paleozoic suture in

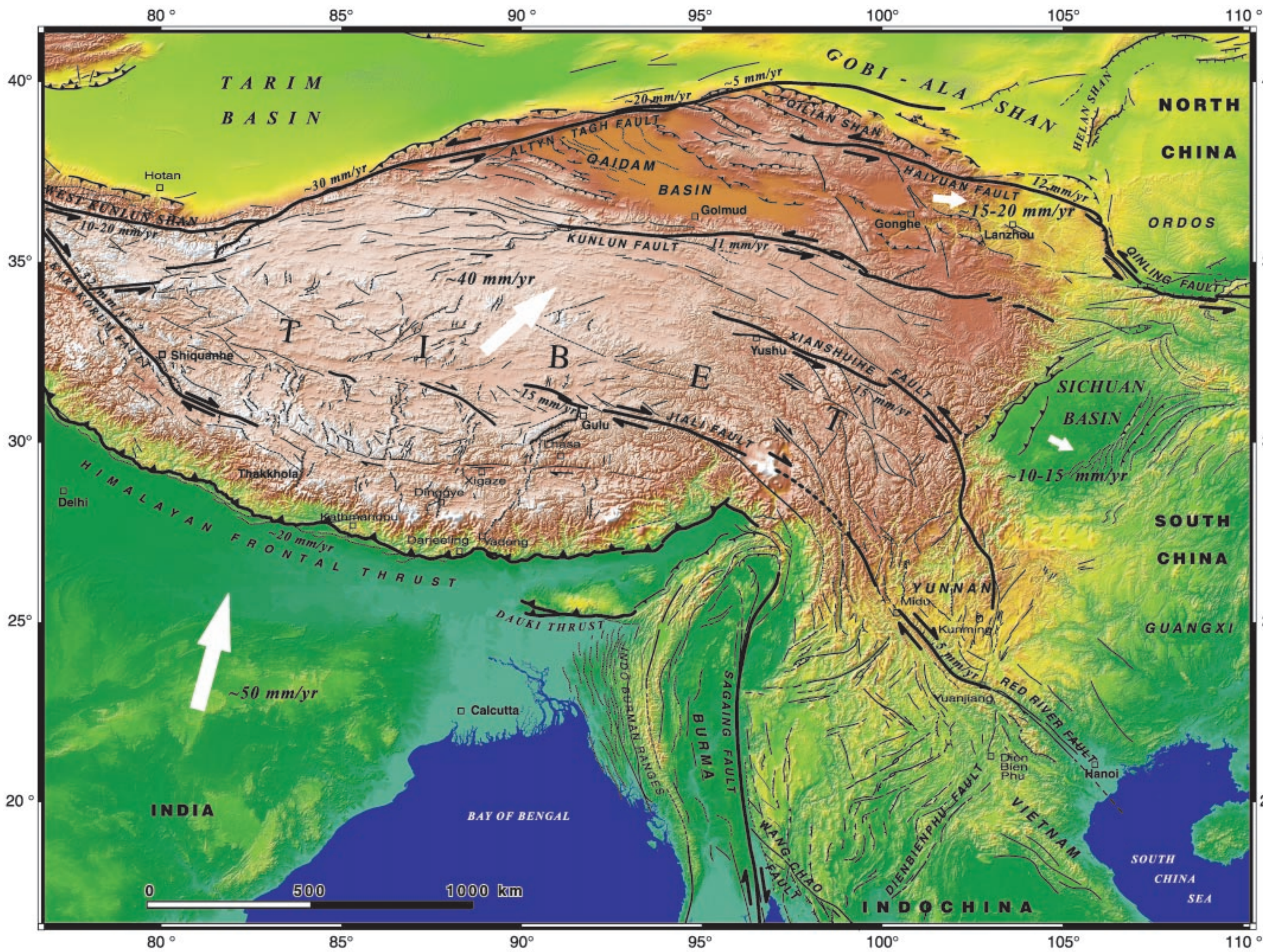

Fig. 1. Topography (*3*) and principal active faults of Tibet and adjacent regions (*1*, *2*, *4*, *12*, *21–27*, *53*, *54*, *56*, *57*, *99*). Bold lines are faults that slip at 5 mm/year or more. Bold numbers indicate rates where known. Thin lines, slower slipping faults. Dashed thin lines, inferred faults. Dotted lines, recent or growing folds. White arrows indicate motions of India, central Tibet, northeasternmost Tibet, and Sichuan relative to Siberia (*56*, *57*, *94*, *100*).

the Altun and Qilian Shan (*48*, *49*), at 93° and 96.5°E respectively, testifies to ~300 km of sinistral offset. To the south, displaced facies transitions of Bajocian deposits in the Qaidam and Tarim Basins suggest that the post-Jurassic offset between 86° and 91°E is greater (400 ± 60 km) (*50*). Yet farther south, the offset of the Permian granitoids of the eastern and western Kunlun reaches 500 to 600 km (*40*, *41*, *51*). The concordant offset of a Cretaceous shear-zone found along the southern edge of the Kunlun implies that this largest displacement postdates ~100 Ma (*52*). The 3 ± 0.5 cm/year, 110 to 5 ka, left-slip rate derived from ^{14}C and ^{10}Be-^{26}Al cosmogenic dating of offset terrace risers and glacial moraines (*53*, *54*) along the central segment of the fault (Fig. 1), further suggests that 500 to 600 km of offset on that segment could have accrued in the last 14 to 24 million years. The eastward decrease in total offset is consistent with propagation of the fault toward the Northeast (*28–30*). Cumulative offsets on the other large sinistral faults of Tibet (Haiyuan, Kunlun, Xianshui He) (Figs. 1 and 2) remain debatable but reach or exceed 100 km (*27*, *55–57*).

Ongoing studies thus indicate that thrusting and sinistral strike-slip faulting have been dominant and equivalent crustal deformation processes in Tibet. The total transpressive shortening taken up by such faults, which appear to have been active during most of the collision span, dwarfs by more than one order of magnitude the total extension across the recent, short-lived normal faults. Comparing the amounts and timing of strain related to either thus shows that the buildup of large-scale Tibetan topography probably had little to do with buoyant rebound and extension at any epoch. Moreover, it is hard to see how gravity-induced outward spreading of a thin, viscous lithospheric sheet might have driven strike-slip motion and overthrusting at the edges of the plateau (*8–10*, *27*, *58*). Rather than being a small Plio-Quaternary addition to the collision process, strike-slip faulting began early on, ~15 Ma or less after the onset of continental impact. Besides, the activation of the large strike-slip faults, which appear to have propagated eastward (*29*, *30*, *43*), was diachronous, starting earlier in the south than in the north (*24–26*, *56*, *57*). The age of strongly folded detrital sediments younger than ~100 Ma also decreases northward across the plateau (*28–30*, *33–37*).

Crust and Mantle Tomography

Seismic studies now provide more information on the bulk velocity structure of the crust and mantle beneath the Tibet plateau. Aniso-

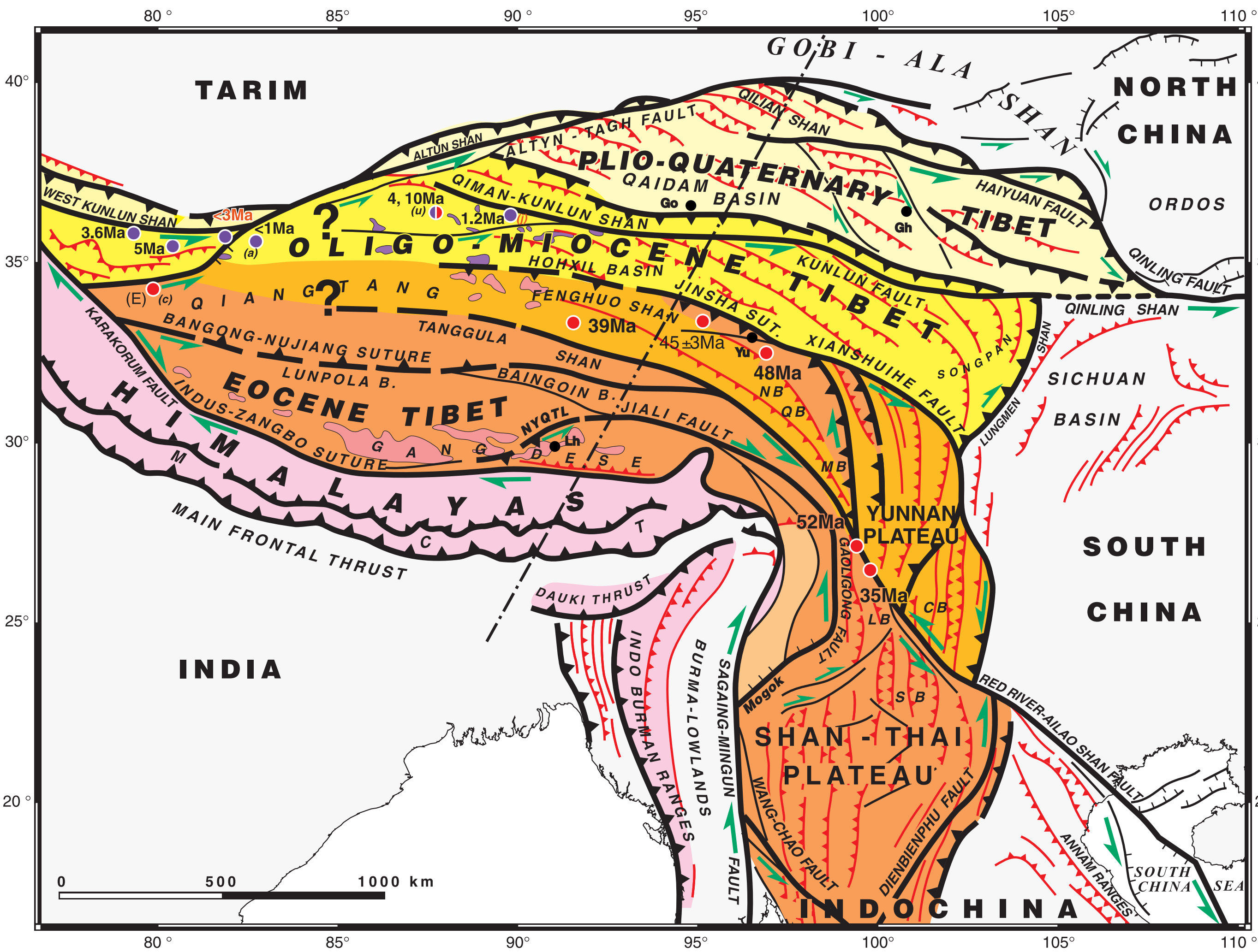

Fig. 2. Simplified map of major tectonic boundaries and Tertiary faults in Tibet, modified from (*21*, *22*, *24–27*, *40*, *41*, *51*, *90*). Bold black lines are major faults and localized shear zones (megathrust or strike-slip) with largest finite offsets, which may extend into lithospheric mantle. Dashed where uncertain. Thin red lines are crustal thrusts. Red and violet circles are Eocene and Plio-Quaternary magmatic centers, respectively, in central Tibet (*80–83*, *90*). Corresponding numbers are ages discussed in text. Patches with deep pink and violet shades schematize other areas with Eocene–Early Miocene and Late Miocene–Quaternary lavas, respectively (*84–86*). Orange to pale yellow shades represent inferred ages of principal plateau-building epochs at expense of Asian crust (*24–26*, *28–30*). Light pink shade south of Zangbo suture and west of Shan plateau indicates thickened Indian crust. Dashed line shows location of section in Fig. 3. Lh, Lhasa. Go, Golmud. Gh, Gonghe. Yu, Yushu. (a) Achikule, (j) Jingyu, (u) Ulugh Mustagh, (c) Changerchar, (E) Eocene. NB, QB, MB, LB, CB, SB, Nangqen, Qamdo, Markham, Lanping, Chuxiong, and Simao basins. MCT, Main central thrust.

tropic inversion of Raleigh- and Love-wave phase-velocities (*59*) shows that, between depths of 100 and 300 km, the mantle is faster, hence colder, under Tibet than under adjacent regions (Fig. 3), corroborating previous inferences (*60–62*). The surface-wave data consequently imply, contrary to local, teleseismic P-wave tomograms along the Golmud-Lhasa profile (Fig. 1) (*63*), which yield only relative velocity contrasts, that low velocities are mostly restricted to the thick crust of the high plateau (*59*, *60*). The origin of the inefficient propagation of high frequency Sn-waves and of the slower Pn-wave velocity between the Tanggula and Kunlun ranges (*64*) may thus also lie at a shallower level (<100 km) than hitherto thought. Widespread lower crustal partial melting (*65*), however, is not required by low velocities. That there might be little such melting, if any, is suggested both by the low V_p/V_s and Poisson's ratios derived from simulated annealing inversion of teleseismic radial receiver functions along the Gonghe-Yushu profile (*66*) (Fig. 1), and by the presence of anhydrous crustal xenoliths in the Pliocene shoshonites of Qiangtang (*67*) (Fig. 2).

Large changes in mantle structure are seen at major crustal boundaries. Beneath the central Altyn Tagh Fault near 91°E, teleseismic tomography reveals a steep, 40-km-wide, low-P-wave velocity anomaly—up to –8% relative to adjacent regions—in the crust and mantle down to 140 km depth, aligned with the surface trace of the fault (*68*). This anomaly is best interpreted to outline a deep, narrow, transpressive shear-zone (*68*), comparable to that now partly exhumed along the Red River. Teleseismic S-wave splitting across the anomaly shows both an increase in delay times of up to 1.3 s, indicative of mantle anisotropy, and a sharp 40° swing of the fast polarization direction in less than 40 km, compatible with sinistral drag (*69*). Both observations argue for localized shear in the continental lithospheric mantle along the Altyn Tagh Fault, rather than for uniform, widespread anisotropic flow beneath Tibet (*70*). Changes in anisotropy across the Karakorum-Jiali fault zone (*1*, *2*) (Fig. 1) have been similarly interpreted to reflect deep-seated shear (*71*).

Taken together, such results are not consistent with the tenets of the soft Tibet paradigm (*9*, *10*, *58*, *70*). First, localized transpressive shear-zones reaching the base of the lithosphere, such as the Altyn Tagh or Red-River Ailao-Shan ought to be little different from plate boundaries, as expected from their great length (>1500 km), fast rates (2.5 to 4 cm/year), and large total offsets (≥500 km) (*21*, *22*, *24–26*, *48–54*). Second, if Tibet's mantle is colder than that of adjacent cratons, upwelling of hot asthenosphere could not have taken place beneath the plateau (Fig. 3). It is thus unlikely that convective removal of thickened lithospheric mantle occurred since the Eocene. Third, and consequently, it is also unlikely that such cold mantle might result from thickening of the lithosphere. For if such a process had taken place, given Tibetan Moho depths (up to 70 to 80 km) (*66*, *72*, *73*), and usually accepted crustal and mantle densities (*10*, *72*, *73*), the average elevation of the plateau, which appears to be isostatically compensated (*10*, *74*), would be appreciably less than 5000 m (*10*). Therefore, allowing for smear due to the low resolution (>350 km) of surface-wave tomography, inward subduction of lithospheric mantle slabs beneath Tibet (*59*) seems to be a more plausible way to account for the high surface-wave velocities observed below 100 km. In short, the crust most likely thickened while the mantle did not, and such thickening must have been decoupled from a more plate-like behavior of the lithosphere underneath (Fig. 3). The inward-dipping interfaces recently imaged by teleseismic receiver functions below about 100 km along the Passcal-Indepth-Gedepth transect (*75*) support this interpretation.

Ongoing Rise of NE Tibet

Nowhere does active overthrusting spread over a greater surface area (~500,000 km^2) than in the NE corner of Tibet. To the south and north, this broad region of coeval mountain building is limited by the Kunlun and Altyn Tagh-Haiyuan fault systems, respectively (Figs. 1 and 2). All the large, 200- to 600-km-long, parallel (N120°E) mountain ranges in between, from the Qiman to the Qilian Shan, appear to grow as ramp anticlines of crustal scale, and most north-facing range-fronts are bounded by active thrusts (*28–30*). Cumulative regional shortening perpendicular to such thrusts (N30°E) appears to have taken place at more than 1.5 cm/year in the last 10 Ma (*28–30*). This rate is only slightly less than that across the Himalayas (*19*, *20*), and comparable to the post-glacial sinistral slip-rates of the Kunlun, Haiyuan, and northern Altyn Tagh faults (>1 and 2

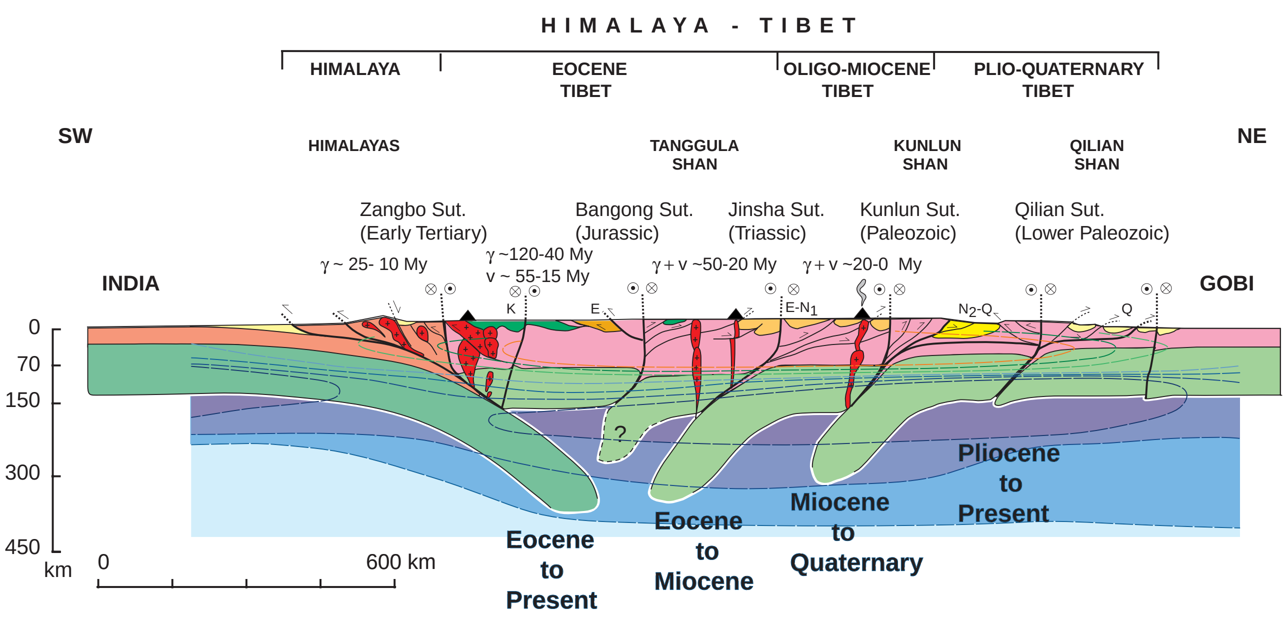

Fig. 3. Schematic lithospheric section of Cenozoic evolution of Himalaya-Tibet orogen. Shades of green represent subducted Indian and Asian lithospheric mantle. Shades of red and pink, Indian and Asian crust, or intrusives. Yellow and dark green shades, ages of sedimentary basins. Relative importance of sedimentary fills is portrayed, but thicknesses are not to scale. Dashed contours (5% intervals) and shades of blue in mantle show variation of $L = \rho V_s^2$ with depth (V_s, shear wave velocity), after (*59*).

cm/a, respectively) (*21*, *22*, *54*, *56*, *57*).

Within the active realm of the collision zone, this region displays telling features. First, there is everywhere an intimate link between the sinistral faults and the generally north-vergent thrusts. Active thrusts along the southern edge of the Qaidam basin (*76*), most of them hidden beneath anticlines folding the about 8-km-thick upper-Miocene to Quaternary sedimentary cover (*28–30*) parallel the Kunlun fault for about 1000 km along strike. This attests to large-scale slip-partitioning, as along oblique subduction zones (Figs. 1 and 2). Thrusts south of the Altyn Tagh fault splay from it at an angle of about 40°, forming a horsetail of grand scale, and seem to young eastward (*28–30*). This suggests that they developed south of the termination of the fault as it propagated northeastward across the Precambrian-Lower Paleozoic Tarim-Qaidam and Gobi-Ala Shan platforms (*28–30*). Present-day slip-rates sum where the thrusts merge with the fault (*28–30*, *77*), as at FFT triple junctions. Such connected thrusting and strike-slip faulting are thus complementary facets of the same deformation process. Mountain building south of the fault results from the slip decrease along it. Rather than postdate crustal thickening (*78*, *79*), strike-slip faulting governs the geometry of thrusting, and participates in driving it.

Second, the main ranges, which typically culminate at elevations between 5500 and 6000 m, ~2000 m lower than Tibet's southern rim, enclose high, flat, 30- to 200-km-wide basins, most of which are undrained. The largest is the Qaidam basin, ~2700 m a.s.l. (Fig. 1). Smaller intermontane basins north of the Qaidam reach elevations in excess of 3000 m. Such high sedimentary flats seem to start as foreland basins, evolve into piggy-backs, and finally become captive of the surrounding relief, as their outwashes are cut off by tectonic uplift of the boundary ranges. At that stage, upstream catchments fill the basins, potentially up to their mountain rims. Such "bathtub infilling" (*28–30*), at work in the Qaidam since the Upper-Miocene, accounts for the exceptionally thick fluvio-lacustrine sedimentary sequence of that age. Basin infill is thus an integral part of the crustal thickening and elevation increase process. Not only does it store mass inside the mountains, slowing down the efficiency of outbound erosion, but it smoothes out regional relief and, together with the unusually broad areal extent of coeval thrusting (*28–30*, *76*), shapes NE Tibet into a broad plateau of uniform height rather than into a higher, narrower, jagged mountain barrier. Hence, at its present size of half a million square kilometers and 3.5- to 4-km average elevation, this northeasternmost corner of the collision highlands provides the best model of a small, still actively growing and rising, Tibet plateau.

Finally, most of the parallel ranges between the basins are less than 40 km wide. They are bounded by segmented thrust faults that slip at only a few millimeters per year. The thrust segments are but a few tens of kilometers long. Such scales and rates imply that the thrusts do not reach into the mantle (*28–30*, *76*, *77*). Size notwithstanding, the overall geometry of faulting and folding is identical to that typical of foreland fold and thrust belts, in which the shortened sedimentary cover is decoupled from the underthrust basement. The Plio-Quaternary shortening and progressive "plateau rise" of this part of Tibet (Figs. 1 and 2) is thus most simply interpreted to reflect the continuing growth of a thick-skinned, crustal accretionary wedge, decoupled from the mantle underneath on a gently south-dipping décollement, probably located near the base of the ductile lower-crust (*28–30*). Hence, in keeping with inferences derived from seismological evidence, probably only the crust thickens, whereas the mantle does not. Given the minimum amount of shortening between the Gobi and Kunlun range, it is likely that the lithospheric mantle of NE Tibet subducts obliquely southwestwards beneath that range to about 200- to 300-km depth (*28–30*), consistent with sinistral slip-partitioning along the range (Figs. 2 and 3).

Diachronous Cenozoic Magmatism

A fraction of Tibet's magmatism, notably volcanism, occurred after India's initial impact onto Asia, mostly inward of the north and south rims of the high plateau (Figs. 2 and 3) (*55*). It was neither widespread and voluminous, nor synchronous (Fig. 2). The volcanism is characterized by high K lavas (shoshonites, latites) and calc-alkaline dacites, trachytes, and rhyolites (*80–86*). The petrology of the rocks implies that the magmas come from partial melting of the subcontinental lithospheric mantle and, to a lesser degree, the crust (*80–86*), but not from strictly asthenospheric or mantle plume sources. The most recent volcanism (≤20 Ma), with K/Ar and Ar/Ar ages mostly between 14 and 8 Ma (*80–84*), forms a patchy belt stretching along the Kunlun mountains between 78° and 93°E. Plio-Quaternary volcanic centers (Fig. 2) are located just south of the Kunlun range. The youngest edifices are closest to the main, northern branches of the Kunlun and Altyn Tagh faults, and two fields (Jingyu Hu, 36°20N and 89°45E, Achikule, 35°40N and 81°30E, ~5000 m a.s.l.; Figs. 1 and 2) have vents untouched by glacial erosion that likely formed in the last 15,000 years. At Ulugh Muztagh, 4-Ma-old rhyolitic tuffs are associated with 10-Ma-old, anatectic granites (*82–84*). The location of recent volcanoes relative to the strike-slip faults is similar to that observed along oblique subduction zones (*87*), but volcanism reaches farther south where the faults splay southeastward into rifts (*1*, *2*, *21*, *22*).

Along the southern edge of the plateau, postcollisional and earlier magmatic episodes overlap (Figs. 2 and 3). U/Pb ages of calkalcaline granitoids in the Gangdese range from 120 to 40 Ma [e.g., (*11*, *45*, *46*, *88*, *89*)]. Volcanism is younger, starting with the Lingzizong ignimbrites at 55 Ma, which probably reflect continental welding (e.g., *40*, *47*), and reaching into the Late Miocene, with most Ar/Ar ages between 26 and 15 Ma (*85*, *86*). There has been no volcanism south of the Zangbo suture and Karakorum fault. Overall, magmatism along Tibet's south rim has been more abundant and longer-lived than in the north. This supports the usually accepted view that unabated subduction of the Indian lithosphere beneath Tibet provided a lasting source of melts north of the suture (Figs. 2 and 3).

Other Tertiary magmatic rocks—calkalcaline granitoids and cogenetic rhyodacites—are found along the summits of the Tanggula range, which stands halfway and highest between the Kunlun and Gangdese mountain belts (*90*). These rocks, which have U/Pb and Ar/Ar ages of 39 to 48 Ma, are much younger than the Triassic and Cretaceous plutons that mark the Mesozoic welding of the central Tibetan collage. But they are roughly coeval with deformed granites with U/Pb ages of 35 to 52 Ma (*45*, *46*) at the west end of the Ailao Shan shear zone and with Paleogene volcanic rocks at the western tip of northern Qiangtang (Changerchar) (Fig. 2) and in the central Pamirs. Together, such Eocene calcalkaline rocks thus mark a third postcollisional magmatic belt cutting the interior of the plateau in half from 80 to 100°E (*90*).

The localization of Cenozoic calkalcaline magmatism along three distinct belts of different ages, following the three principal topographic ranges north of the Zangbo suture (Gangdese, Tanggula, Kunlun), roughly parallel to the Himalayas, is more consistent with melt sources related to subduction beneath the ranges (*28–30*, *67*, *80*, *81*, *90*) (Fig. 3) than with wholesale convective thinning of the lithospheric mantle. The process operating since the Miocene along and north of the Kunlun edge of the high plateau appears to have had an earlier, Eocene-Oligocene equivalent along the Tanggula range (Fig. 3), which may have marked at the time the northern boundary of a smaller plateau.

That the growth of central and southern Tibet occurred in distinct stages by mechanisms similar to that now observed in NE Tibet is further supported by structural and kinematic evidence. The relation between the Kunlun fault and the thrusts that cut and fold the Eocene-Oligocene red beds south of the

Kunlun range (*33–37*, *55*) is comparable to that of the Plio-Quaternary thrusts that splay southeastward at ~40° from the Altyn Tagh Fault (Fig. 2) (*28–30*). A similar transpressive geometry is observed for thrusts and folds—now trending roughly NS—in the older, Cretaceous-Eocene red beds southwest of the—now SE-striking—Red River (*24–26*) and Xianshui He (*27*) faults (Fig. 2). This relationship implies that, between the Paleogene and Miocene, the large strike-slip faults of central and southeastern Tibet played a role analogous to that of the Altyn Tagh and Kunlun faults in the more recent growth of NE Tibet. West of 97°E, the Kunlun, Xianshui He, and Red River faults roughly follow the ultramafic rock girdles that mark the Kunlun-Anyemaqen, Jinsha, and Bangong-Nujiang sutures, respectively. This geometry suggests that the three faults reactivated the three weakest lithospheric cuts in the Tibetan collage, along which shear in the mantle could develop into oblique subduction.

Throughout the collision process, therefore, after India's impact onto Asia about 55 Ma ago, the same mechanism, coupling sinistral strike-slip faulting and accretionary thrust-wedge growth in the crust with oblique lithospheric mantle subduction deeper down, may have repeated itself, step after step toward the north, leading to the successive rise of three plateaus (Figs. 1 to 3). Soon after impact, the Bangong, then the Jinsha sutures would have been reactivated as mantle megathrusts, near the northern edge of a zone of high relief that grew eastward while escaping in this same direction. The Tanggula, then the Fengguo ranges, and the Red-River, then the Xianshuihe shear-zones would have formed at that time, coevally with transpressive folding and thrusting (*24–26*) and infilling of intervening basins in southern Tibet, southern Sichuan, Yunnan, and the Shan-Thai plateau (Fig. 2). The southern and northeastern limits of this early Tibet plateau probably followed the Zangbo and Jinsha sutures, respectively, because Eocene Palmacea are not found in between (*91*). Later, in the Oligocene and Miocene, oblique growth and extrusion of the central plateau, between the Tanggula and Kunlun Shan, would have superseded the earlier relief rise in the south (*26*, *29*) (Figs. 2 and 3). Asian lithospheric mantle would have started to subduct southward along the Kunlun-Anyemaqen suture. The Kunlun fault would have propagated eastward (*29*), and the Hoxhil-basin and Songpan wedges would have become incorporated into the highlands. Resumed uplift of the Lungmen Shan (*92*) and folding of the Paleozoic-Mesozoic sediment cover of the South China craton, all the way to eastern Sichuan and Guangxi (*93*), were likely coeval with that second plateau growth phase. The third phase of areal growth and rise, still in progress, probably started in the Late Miocene, with branches of the Altyn Tagh fault propagating past and around the Qilian Shan to the Haiyuan Fault (*28–30*, *56*, *57*), shifting the plateau rim to the edge of the Gobi and circumventing the Qaidam and Gonghe basins (Figs. 1 to 3).

Summary and Discussion

Although the three-phase Tibet growth model presented here remains conjectural, it brings many large-scale features of Tibet's Tertiary history, structure, and topography into a consistent framework. Oblique subduction of Asian lithospheric mantle is a mechanism that can viably coinvolve extrusion and crustal thickening. It can account for markedly asymmetric growth of relief toward the east, and for large amounts of both localized sinistral shear and coeval, distributed crustal thickening. Sequential, northward reactivation of sutures as India penetrated into Asia is what the opposite, southward vergence of Phanerozoic welding (*48*, *88*) leads to expect (*29*). The resulting, stepwise, diachronous rise of the Tibetan highlands accounts for the differences in present-day relief and tectonic regimes (Fig. 1). The highest, flattest, and smoothest part of Tibet (*3*) is the central, Oligo-Miocene plateau, mature but still sheltered, especially in the west, from headward erosion. It lies between the immature, still-growing NE plateau and the early SE plateau, now more deeply dissected. The most vigorously rising thrust-ranges along the eastern rim of Tibet lie north of the Kunlun fault (*28–30*). Shortening along the Lungmen Shan, by contrast, is now modest, despite continuing erosional unroofing (*92*, *94*). Farther south, the edge of the Yunnan plateau has become a site of tectonic inversion, with small-scale, extensional bookshelf faulting, and with normal faults reactivating early Tertiary thrusts (*24–26*, *95*). That, unlike the Altyn Tagh fault, the large strike-slip faults of eastern Tibet seem to die out westward into the least explored part of the plateau (Fig. 2) is also easily accounted for. Their western stretches were probably cut off and superseded by more northerly faults, then smothered by basin infilling, as were early thrusts in the plateau interior. That the longest, fastest slipping shear zones form barriers to recent thrust or normal faults (Figs. 1 and 2) supports the inference that these zones extend deep into the lithospheric mantle. Conversely, the slower-slipping thrust or normal faults that cross neither the Red River, Kunlun, and Altyn Tagh Faults, nor the Bangong and Zangbo sutures, probably do not extend beneath the décollements that likely underlie much of the thickened crust of Tibet.

The stepwise growth scenario requires that a form of hidden Plate Tectonics has been operating beneath the deforming Asian crust. It seems unlikely that the mantle of Tibet ever behaved as a fluid, and that thickening of a viscous sheet coinvolving crust and mantle ever provided enough buoyancy to drive subsequent deformation (*9*, *10*, *58*). Instead, boundary forces along the Himalayas and the eastern edge of the Asian plate resulted in stresses sufficient to reactivate weakly welded sutures and to shear anew the Asian lithosphere along narrow zones, isolating coherent mantle blocks (*40*, *41*, *51*). Successive, oblique mantle subduction zones were thus created (*28–30*, *96*), leading to the growth of crustal accretionary wedges, decoupled from the mantle in the weak lower crust. Subduction of Asian mantle slabs, once initiated, may have played a dynamic, feedback role in maintaining the continued growth and rise of the plateau. Tectonic damming of catchments and basin infill also played a key role in storing debris and slowing outbound erosion. Along major block boundaries, coeval crustal deformation was partitioned between steep strike-slip shear zones and gently dipping décollements, both chief elements of long-lasting collision. That the mantle part—initially >75%—of the lithosphere did not thicken may explain why two-dimensional, analog-model experiments have been the only ones to predict successfully the existence of such first-order Asian tectonic structures as the Red River and Altyn Tagh faults (*40*, *41*, *51*). Finally, a stepwise rise of different parts of Tibet makes postulated links between climate changes and tectonics (*10*) more plausible. Different stages of growth of the plateau could have contributed to trigger or enhance different climatic effects at different times, with thresholds in surface area being at least as important as height in shifting atmospheric circulation patterns (*97*, *98*).

The main tenets of this model require testing. None of the postulated mantle subduction zones has yet been convincingly imaged. Regional paleo-elevations and uplift histories are mostly unknown. Three phases of growth may be discerned, but the boundaries of early accretionary wedges within the plateau, particularly in the west, remain uncertain. Deformation ages in eastern Tibet, western Sichuan, and northern Yunnan are also poorly known (*27*, *90*, *92*). Whether large Tertiary basins existed in eastern Songpan is unclear, although stronger glacial and fluvial erosion in this most humid part of the plateau could have abraded them out in the last 10 million years. The dips of resumed Tertiary subductions along Tibet's southern sutures remain questionable (*90*). But the mechanism at the core of the stepwise growth scenario provides an alternative to the soft Tibet model that does not leave out first-order features of the time-dependent rise of the plateau. What makes the behavior of the continental lithosphere singular is probably less some overall, fluid-like weakness than structural contrasts in rheology and the ease with which large-scale shear zones localize and propagate.

References and Notes

1. R. Armijo, P. Tapponnier, J. L. Mercier, H. Tong-Lin, *J. Geophys. Res.* **91**, 13803 (1986).
2. R. Armijo, P. Tapponnier, T. Han, *J. Geophys. Res.* **94**, 2787 (1989).
3. E. Fielding, B. Isacks, M. Barazangi, C. C. Duncan, *Geology* **22**, 163 (1994).
4. P. Molnar, P. Tapponnier, *J. Geophys. Res* **83**, 5361 (1978).
5. P. Tapponnier *et al.*, *Nature* **294**, 410 (1981).
6. P. Molnar, H. Lyon-Caen, *Geophys. J. Int.* **99**, 123 (1989).
7. M. Coleman, K. Hodges, *Nature* **374**, 49 (1995).
8. S. L. Chung *et al.*, *Nature* **394**, 769 (1998).
9. P. C. England, G. A. Houseman, *J. Geophys. Res.* **94**, 17561 (1989).
10. P. Molnar, P. England, J. Martinod, *Rev. Geophys.* **31**, 357 (1993).
11. T. M. Harrison, P. Copeland, W. S. F. Kidd, A. Yin, *Science* **255**, 1663 (1992).
12. P. Tapponnier, P. Molnar, *J. Geophys. Res.* **82**, 2905 (1977).
13. T. M. Harrison, P. Copeland, W. S. F. Kidd, O. M. Lovera, *Tectonics* **14**, 658 (1995).
14. C. N. Garzione *et al.*, *Geology* **28**, 339 (2000).
15. H. Lyon-Caen, P. Molnar, *Geophys. Res. Lett.* **11**, 1251 (1984).
16. W. Zhao *et al.*, *Nature* **366**, 557 (1993).
17. L. Ratschbacher, W. Frisch, G. Liu, C. Ghen, *J. Geophys. Res.* **99**, 19917 (1994).
18. R. McCaffrey, J. Nabelek, *Geology* **26**, 691 (1998).
19. J. Lavé, J. P. Avouac, *J. Geophys. Res.* **105**, 5735 (2000).
20. R. Bilham, K. Larson, J. Freymuller, *Nature* **386**, 61 (1997).
21. J. Van der Woerd *et al.*, *Geology* **26**, 695 (1998).
22. J. Van der Woerd *et al.*, *Geophys. Res. Lett.* **27**, 2353 (2000).
23. A. Yin *et al.*, *Geology* **27**, 787 (1999).
24. P. H. Leloup *et al.*, *Tectonophysics* **251**, 3 (1995).
25. R. Lacassin *et al.*, *Tectonics* **15**, 605 (1996).
26. R. Lacassin *et al.*, *J. Geophys. Res.* **102**, 10013 (1997).
27. E. Wang *et al.*, *Geol. Soc. Am. Spec. Paper* **327**, 1-108 (1998).
28. P. Tapponnier *et al.*, *Earth Planet. Sci. Lett.* **97**, 382 (1990).
29. B. Meyer *et al.*, *Geophys. J. Int.* **135**, 1 (1998).
30. F. Metivier, Y. Gaudemer, P. Tapponnier, B. Meyer, *Tectonics* **17**, 823 (1998).
31. J. Achache *et al.*, *J. Geophys. Res.* **89,** 10311 (1984).
32. J. Besse, V. Courtillot, J. P. Pozzi, M. Westphal, Y. X. Zhou, *Nature* **311**, 621 (1984).
33. C. Chang, *et al.*, *Nature* **323**, 501 (1986).
34. W. S. F. Kidd *et al.*, *Philos. Trans. R. Soc. London* **327**, 287 (1988).
35. M. P. Coward *et al.*, *Philos. Trans. R. Soc. London* **327**, 307 (1988).
36. Z. Liu, C. Wang, *Sediment. Geol.*, in press.
37. ———, H. Yi, *J. Sediment. Res.*, in press.
38. A. Yin *et al.*, *J. Geophys. Res.* **99**, 18175 (1994).
39. A. Yin *et al.*, *Geology* **27**, 787 (1999).
40. P. Tapponnier, G. Peltzer, R. Armijo, *Geol. Soc. Spec. Publ.* **19**, 115 (1986).
41. P. Matte *et al.*, *Earth Planet. Sci. Lett.*, **142**, 311 (1996).
42. Z. Yang, J. Besse, *Earth Planet. Sci. Lett.* **117**, 525 (1993).
43. A. Briais, P. Patriat, P. Tapponnier, *J. Geophys. Res.* **98**, 6299 (1993).
44. T. M. Harrison *et al.*, in *Tectonic Evolution of Asia*, A. Yin and T. M. Harrison, Eds. (Cambridge Univ. Press, New York, 1996), pp. 208–226.
45. U. Schärer *et al.*, *Earth Planet. Sci. Lett.* **97**, 65 (1990).
46. L. S. Zhang, U. Schärer, *Contrib. Mineral. Petrol.* **134**, 67 (1999).
47. J. J. Jaëger, V. Courtillot, P. Tapponnier, *Geology* **17**, 316 (1987).
48. Z. Xu, in 15th Himalaya-Karakoram-Tibet Workshop, Chengdu, 21 to 24 April 2000, Earth Sciences Frontiers (China Univ. of Geosciences, Beijing, 2000), vol. 7, p. 231.
49. E. Sobel, N. Arnaud, *Tectonics* **18**, 64 (1999).
50. B. D. Ritts, U. Biffi, *G.S.A. Bull.* **112**, 61 (2000).
51. G. Peltzer, P. Tapponnier, *J. Geophys. Res.* **93**, 15085 (1988).
52. N. Arnaud *et al.*, in preparation.
53. A.-S. Mériaux *et al.*, *EOS Trans.* (AGU Fall meeting), **81,** 1137 (2000).
54. F. J. Ryerson *et al.*, *EOS Trans.* (AGU Fall meeting) **80**, 1008 (1999).
55. Geological Map of Qinghai-Xizang Plateau and Adjacent Areas (scale: 1/1,500,000) (Geology Publishing House, Beijing, 1988).
56. Y. Gaudemer *et al.*, *Geophys. J. Int.* **120**, 599 (1995).
57. C. Lasserre *et al.*, *J. Geophys. Res.* **104**, 17633 (1999).
58. P. England, P. Molnar, *Science* **278**, 647 (1997).
59. D. Griot, J. P. Montagner, P. Tapponnier, *J. Geophys. Res.* **103**, 21215 (1998).
60. L. Bourjot, B. Romanowicz, *Geophys. Res. Lett.* **19**, 881 (1992).
61. J. Revenaugh, S. A. Sipkin, *J Geophys. Res.* **99**, 21911 (1994).
62. R. Zeng, Z. Ding, Q. Wu, *Pure Appl. Geophys.* **145**, 425 (1995).
63. G. Wittlinger *et al.*, *Earth Planet. Sci. Lett.* **139**, 263 (1996).
64. D. McNamara, T. Owens, W. Walter, *J. Geophys. Res.* **100**, 22215 (1995).
65. T. J. Owens, G. Zandt, *Nature* **387**, 37 (1997).
66. G. Wittlinger *et al.*, in preparation.
67. R. Hacker *et al.*, *Science* **287**, 2463 (2000).
68. G. Wittlinger *et al.*, *Science* **282**, 74 (1998).
69. G. Herquel *et al.*, *Geophys. Res. Lett.* **26**, 3225 (1999).
70. W. E. Holt, *Geology* **28**, 67 (2000).
71. W. C. Huang *et al.*, *J. Geophys. Res.* **105**, 27979 (2000).
72. A. Hirn *et al.*, *Nature* **307**, 23 (1984).
73. A. Hirn *et al.*, *Nature* **307**, 25 (1984).
74. Y. Jin, M. K. McNutt, Y. Zhu, *Nature* **371**, 669 (1994).
75. G. Kosarev *et al.*, *Science* **283**, 1306 (1999).
76. W. P. Chen, C. Y. Chen, J. L. Nabelek, *Tectonophysics* **305**, 165 (1999).
77. J. Van der Woerd *et al.*, *Tectonics*, in press.
78. B. C. Burchfiel *et al.*, *Geology* **17**, 448 (1989).
79. E. Wang, *Earth Planet. Sci. Lett.* **150**, 55 (1997).
80. W. Deng, *Chin. J. Geochem.* **10**, 140 (1991).
81. N. O. Arnaud *et al.*, *Earth Planet. Sci. Lett.* **111**, 351 (1992).
82. B. C. Burchfiel *et al.*, *Earth Planet. Sci. Lett.* **94**, 57 (1989).
83. S. Turner *et al.*, *J. Petrol.* **37**, 45 (1996).
84. J. Yang, Z. Xu, W. Bai, R. Zhao, *Contin. Geodyn.* **2**, 1 (1997).
85. C. Coulon, H. Maluski, C. Bollinger, S. Wang, *Earth Planet. Sci. Lett.* **79**, 281 (1986).
86. C. Miller *et al.*, *J. Petrol.* **40**, 1399 (1999).
87. K. Sieh, D. Natawidjaja, *J. Geophys. Res.* **105**, 28295 (2000).
88. C. J. Allègre *et al.*, *Nature* **307**, 17 (1984).
89. F. Debon, P. Le Fort, S. M. F. Sheppard, J. Sonet, *J. Petrol.* **27**, 219 (1986).
90. F. Roger *et al.*, *Terra Nova* **12**, 102 (2000).
91. T. Li, *Tectonophysics* **260**, 45 (1996).
92. D. Arne *et al.*, *Tectonophysics* **280**, 239 (1997).
93. D. Yuan, 1st International Conference on Geomorphology, Manchester, 15 to 21 September 1985.
94. R. King *et al.*, *Geology* **25**, 1279 (1997).
95. F. Wu, P. Wang, *Geology* **16**, 153 (1988).
96. M. Mattauer, *J. Geol. Soc. London Spec. Publ.* **19**, 37 (1986).
97. G. Ramstein, F. Fluteau, J. Besse, S. Joussaume, *Nature* **386**, 788 (1997).
98. F. Fluteau, G. Ramstein, J. Besse, *J. Geophys. Res.* **104**, 11995 (1999).
99. A. Replumaz, R. Lacassin, P. Tapponnier, P. H. Leloup, *J. Geophys. Res.* **106**, 819 (2001).
100. J. P. Avouac, P. Tapponnier, *Geophys. Res. Lett.* **20**, 895 (1993).

101. The concepts presented here benefited from work and discussions with R. Armijo, J. P. Avouac, J. Besse, L. Bourjot, M. Brunel, Y. Chen, J. P. Cogné, V. Courtillot, Y. Gaudemer, S. Gilder, D. A. Griot, G. King, R. Lacassin, C. Lasserre, P. H. Leloup, B. Liu, Q. Liu, X. Liu, J. Malavieille, M. Mattauer, F. Metivier, A. S. Meriaux, J. P. Montagner, G. Peltzer, G. Poupinet, A. Replumaz, F. J. Ryerson, J. Van der Woerd, X. Xu, Z. Yang, among others. The many field trips to most parts of Tibet over the years were unfailingly supported by Institut National des Sciences de l'Univers (CNRS, Paris), and their logistics, by the Ministry of Lands and Resources, the National Science Foundation of China, Academia Sinica and the Seismological Bureau of China (Beijing). P.T. is grateful to the California Institute of Technology, where part of this paper was written while he was on sabbatical as visiting professor. A. C. Morillon is responsible for the quality of the figures. This is Institut de Physique du Globe de Paris contribution no. 1778.